Journal of Achievements in Materials and Manufacturing Engineering
VOLUME 55
ISSUE 2
December
2012

Structure and magnetic properties of $Fe_{56}Co_7Ni_7B_{20}Nb_{10}$ metallic glasses

S. Lesz [a,*], M. Nabiałek [b], R. Nowosielski [a]
[a] Institute of Engineering Materials and Biomaterials,
Silesian University of Technology, ul. Konarskiego 18a, 44-100 Gliwice, Poland
[b] Institute of Physics, Faculty of Materials Processing Technology and Applied Physics,
Czestochowa University of Technology, Al. Armii Krajowej 19, 42-200 Częstochowa, Poland
* Corresponding e-mail address: sabina.lesz@polsl.pl

Received 15.10.2012; published in revised form 01.12.2012

Materials

ABSTRACT

Purpose: This paper presents results of investigation of structure and magnetic properties of $Fe_{56}Co_7Ni_7B_{20}Nb_{10}$ metallic glasses prepared from industrial raw materials. The investigated samples were cast in form of the ribbons. Ribbons were prepared by the single copper roller melt spinning method. The casting conditions include linear speed of copper roller: ν = 18 and ν = 20 m/s and ejection over-pressure of molten alloy: p = 0.02 MPa.

Design/methodology/approach: The structure was characterized by X-ray diffraction (XRD) method, transmission electron microscope (TEM), scanning electron microscope (SEM). The magnetic properties contained, coercive force H_c, initial magnetic permeability μ_i and magnetic after-effects $\Delta\mu/\mu$ measurements were determined by the coercivemeter and with the use of automatic device for measurements magnetic permeability, respectively. Magnetic hysteresis loops were measured with a vibrating sample magnetometer (VSM) under an applied field up to 2 T. Magnetic properties of saturation magnetization - M_s was determined from achieved magnetic hysteresis loops. Hysteresis loops, recorded using a computer controlled DC hysteresis loop tracer, were used to obtain hysteresis parameters.

Findings: The XRD and TEM investigations revealed that the studied ribbons were amorphous. The SEM images showed that studied fractures morphology of ribbons is changing from smooth fracture inside with few veins network in surface freely solidified (shining surface). Character of fracture morphology revealed ductile character of $Fe_{56}Co_7Ni_7B_{20}Nb_{10}$ ribbons with vein pattern morphology, typical for amorphous alloys. The detailed analysis of data of magnetic properties i.e. M_s, μ_i and H_c allow to classify the alloy in as quenched state as a soft magnetic material.

Research limitations/implications: The results can give more details to understand the relationship between structure and magnetic properties. Thus can be useful for practical application of these alloys.

Practical implications: The Fe, Co, Ni-based metallic glasses due to their properties such as excellent magnetic properties are the most attractive and promising for the future applications as new prominent class of engineering and functional material. Thin ribbons of magnetic metallic glasses are currently used in transformer cores, in magnetic sensors, and for magnetic shielding. Higher thicknesses would be useful particularly for the latter two applications.

Originality/value: The applied investigation methods are suitable to determine the changes of structure and soft magnetic properties of examined $Fe_{56}Co_7Ni_7B_{20}Nb_{10}$ metallic glasses with function of sample thickness.

Keywords: Metallic glasses; Structure, Magnetic properties

Reference to this paper should be given in the following way:
S. Lesz, M. Nabiałek, R. Nowosielski, Structure and magnetic properties of $Fe_{56}Co_7Ni_7B_{20}Nb_{10}$ metallic glasses, Journal of Achievements in Materials and Manufacturing Engineering 55/2 (2012) 270-274.

1. Introduction

Metallic glasses have been drawing increasing attention due to their scientific and engineering significance (Inoue, 2010). The metallic glasses (also often referred to as glassy alloys or amorphous alloys) emerged some 50 years ago, defying the expectation that solid metallic states would always be crystalline due to the nature of metallic bonding (Kovalenko, 2001). Metallic glasses offer attractive benefits, combining some of the desirable properties of conventional crystalline metals and the formability of conventional oxide glasses. The absence of grain boundaries in glassy alloys contributes to unique combinations of magnetic (such as high saturation magnetization (M_s) and initial magnetic permeability (μ_i), low coercive force (H_c) (Gutfleisch, 2011), mechanical (such as high strength, high specific strength, large elastic strain limit, ductility) electrical and chemical properties (Greer, 2007).

During the last decades, metallic glasses have been discovered in a wide range of alloys. The first synthesis of an amorphous phase was performed for an $Au_{75}Si_{25}$ alloy by Duwez's group in 1960 (Klement, 1960). The studies on the development of amorphous alloy tapes in Fe- , Co- and Ni-based alloy systems were made for several years since 1970 (Inoue, 1998), (Shen, 2007). Many researches were nearly concentrated on the subject of magnetic properties because of potential magnetic applications of Fe-, Co- and Ni-based metallic glasses. The mechanical properties of metallic glasses are also very important for their applications as structural materials. Recently, with the aim at searching for a Fe-based ferromagnetic glassy alloy system with high strength as well as good soft-magnetic properties, it has been found that $[(Fe_{0.8}Co_{0.1}Ni_{0.1})_{0.75}B_{0.2}Si_{0.05}]_{96}Nb_4$ glassy alloy exhibits super-high strength - σ_f of over 4000 MPa and some ductile strain up to ε=0.005, combined with good soft-magnetic properties (Inoue, 2004).

Alloy design strategies using high purity raw materials and novel elements to produce metallic glasses may not be the most economical approach to developing Fe-, Co, Ni-based metallic glasses for the commercial applications (Liu, 2004), (Sun, 2012). In 2007, Jia et al. found that the $Fe_{36}Co_{36}B_{19.2}Si_{4.8}Nb_4$ have been successfully prepared by using commercial raw materials (Jia, 2007).

This paper presents results of investigation of structure and magnetic properties of $Fe_{56}Co_7Ni_7B_{20}Nb_{10}$ metallic glasses prepared from industrial raw materials. The precursor of investigated alloy was $[(Fe_{0.8}Co_{0.1}Ni_{0.1})_{0.75}B_{0.2}Si_{0.05}]_{96}Nb_4$ glassy alloy, which have been prepared by Inoue from the high purity raw materials (Inoue, 2004). More details about magnetic and mechanical properties and thermal stability of the $[(Fe,Co,Ni)_{0.75}B_{0.2}Si_{0.05}]_{96}Nb_4$ glassy alloys are presents in Table 1 (Shen, 2007).

2. Material and method

2.1. Test material

Investigations were carried out on amorphous ribbons with compositions of $Fe_{56}Co_7Ni_7B_{20}Nb_{10}$. The alloy compositions represent nominal atomic percent. The Fe-based master alloy ingots were prepared by arc melting the mixtures of the Fe-B , Fe-Nb starting alloys and pure Fe, Co, Ni metals in an argon atmosphere.

The investigated samples were cast in form of the tapes with thicknesses from t=0.07 to t=0.15 mm and width of w=0.85 and w=1.95 mm. Ribbons were prepared by the single copper roller melt spinning method. The melt-spinning technique was noticed to be appropriate for the production of amorphous alloy tapes with thickness - t ranging from t=70 to t=150 µm. The casting conditions include linear speed of copper roller: v= 18 and v=20 m/s and ejection over-pressure of molten alloy: p=0.02 MPa.

2.2. Methodology

The structure of the ribbons was examined by X-ray diffraction (XRD) method, transmission electron microscope (TEM), scanning electron microscope (SEM). The X-ray method has been performed by the use of diffractometer X-Pert PRO MP with filtered Co-Kα radiation (λ=0.17888 nm) in Bragg-Brentano geometry. In order to conduct structural study, the electron microscope TESLA BS 540 of 100000× magnitude was used. The morphology of fracture surfaces after decohesion was observed in scanning electron microscope ZEISS SUPRA 25.

The magnetic properties contained, coercive force - H_c, initial magnetic permeability - μ_i (at force H≈0.5 A/m and frequency f≈1 kHz) and magnetic after-effects - $\Delta\mu/\mu$ measurements were determined by the coercivemeter and with the use of automatic device for measurements magnetic permeability, respectively (PN-IEC 60050-121:2000). Where $\Delta\mu=\mu(t_1=30\text{ s})-\mu(t_2=1800\text{ s})$, μ is the initial magnetic permeability measured at time t after demagnetisation (Kronmüller, 1983), (Lesz, 2008).

Magnetic hysteresis loops were measured with a vibrating sample magnetometer (VSM) under an applied field up to 2 T. Magnetic properties of saturation magnetization - Ms was determined from achieved magnetic hysteresis loops. Hysteresis loops, recorded using a computer controlled DC hysteresis loop tracer, were used to obtain hysteresis parameters (Lesz, 2011).

2.3. Results and discussion

It was found from the obtained results of structural studies performed by X-ray diffraction (XRD) that the structure of the ribbons with thickness of both t=0.07 mm and t=0.15 mm of $Fe_{56}Co_7Ni_7B_{20}Nb_{10}$ alloy consists of amorphous phase. Only broad peak without any crystalline peaks can be seen for the all of ribbons (Fig. 1). Obtained results of structural studies performed by XRD are corresponding with the TEM micrograph (Fig. 2, 3). The diffraction pattern taken from the small region consists only of halo rings, and no appreciable reflection spots of crystalline phases are seen (Fig. 2, 3). Character of fracture morphology revealed ductile character of $Fe_{56}Co_7Ni_7B_{20}Nb_{10}$ ribbons with vein pattern morphology, typical for amorphous alloys. Morphology is changing from smooth fracture inside with few veins network in surface freely solidified (shining surface) (Fig. 4, 5).

Table 1.
Magnetic (M_s- saturation magnetization, μ_e - effective permeability, H_c - coercive force, T_c - Curie temperature) and mechanical properties (E-Young's modulus, σ_f - fracture strength, ε - plastic strain, HV - Vickers hardness), thermal stability (T_g - glass transition temperature, $\Delta T_x(=T_x-T_g)$ - supercooled liquid region, T_g/T_m - the reduced glass transition temperature) of the cast $[(Fe_{0.8}Co_{0.1}Ni_{0.1})_{0.75}B_{0.2}Si_{0.05}]_{96}Nb_4$ glassy alloy

Magnetic properties				Mechanical properties				Thermal stability		
M_s [T]	μ_e	H_c [A/m]	T_c [K]	E [GPa]	σ_f [MPa]	ε	HV	T_g [K]	ΔT_x [K]	T_g/T_m
1.1	16 000	3.0	613	208	4225	0.005	1230	818	55	0.606

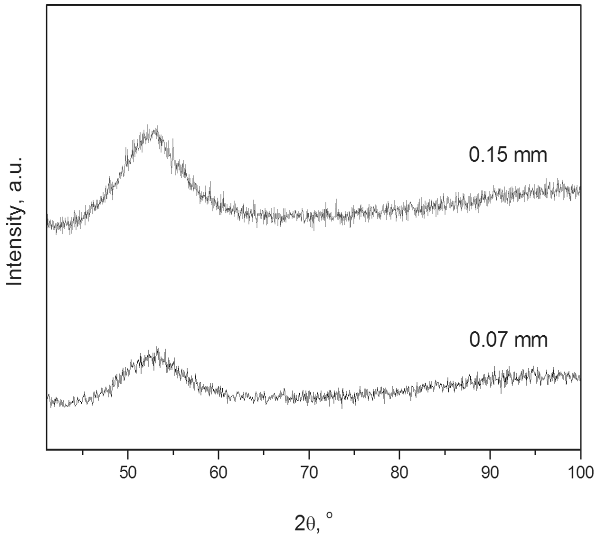

Fig. 1. X-ray diffraction pattern of $Fe_{56}Co_7Ni_7B_{20}Nb_{10}$ ribbons with thickness of t=0.07 mm and t=0.15 mm

The results of magnetic properties measurements of the investigated ribbons of $Fe_{56}Co_7Ni_7B_{20}Nb_{10}$ alloys have been presented in the Table 2 and Fig. 6a, b. Fig. 6 shows hysteresis μ_0M-μ_0H loops of the $Fe_{56}Co_7Ni_7B_{20}Nb_{10}$ glassy ribbons with thickness of t=0.07 mm (a) and t=0.15 mm (b). As shown in Figure 6, the saturation magnetization - M_s of the $Fe_{56}Co_7Ni_7B_{20}Nb_{10}$ ribbons with thickness of t=0.07 mm and t=0.15 mm are 0.89 and 0.79 T, respectively. The slight decrease in the M_s of the loops are considered to be caused by the demagnetization field resulting from the large thickness of the samples (Inoue, 2003). The detailed analysis of data of magnetic properties i.e. M_s, μ_i and H_c allow to classify the alloy in as quenched state as a soft magnetic material (Table 2). The ribbons with thickness of t=0.07 mm have better magnetic properties (H_c=4.0 A/m, μ_i=1300, $\Delta\mu/\mu$=1.1, Table 2) than ribbons with thickness of t=0.15 mm (H_c=3.2 A/m, μ_i=1100, $\Delta\mu/\mu$=8.4, Table 2) of $Fe_{56}Co_7Ni_7B_{20}Nb_{10}$ alloy. This suggest that the casting conditions have influence on microvoids content and thereby on magnetic properties. These excellent magnetic properties (Table 2) lead us to expect that the Fe-based amorphous alloy could be used as a new engineering and functional material intended for parts of inductive components (e.g. micromotors, radio wave clock antennas, watch gears, and other applications).

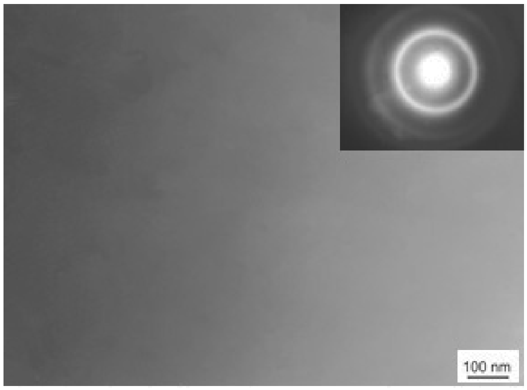

Fig. 2. TEM micrograph and electron diffraction pattern of selected area of $Fe_{56}Co_7Ni_7B_{20}Nb_{10}$ ribbons with thickness of t=0.07 mm

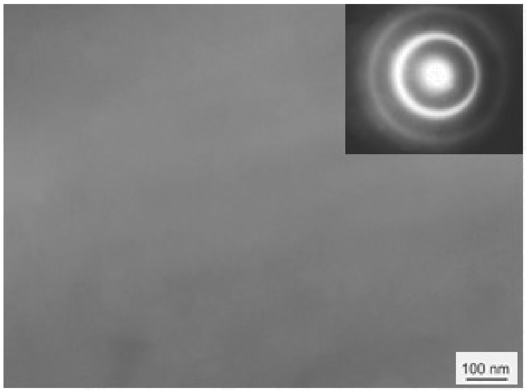

Fig. 3. TEM micrograph and electron diffraction pattern of selected area of $Fe_{56}Co_7Ni_7B_{20}Nb_{10}$ ribbons with thickness of t=0.15 mm

Table 2.
Magnetic properties (μ_i - initial magnetic permeability, $\Delta\mu/\mu$ - magnetic after effects, H_c - coercivity, M_s - saturation magnetization) of $Fe_{56}Co_7Ni_7B_{20}Nb_{10}$ ribbons with thickness of t=0.07 mm and t=0.15 mm (Shen, 2007)

Thickness of ribbons	Magnetic properties			
t [mm]	μ_i	$\Delta\mu/\mu$ [%]	H_c [A/m]	M_s [T]
0.07	1300	1.1	4.0	0.89
0.15	1100	8.4	3.2	0.79

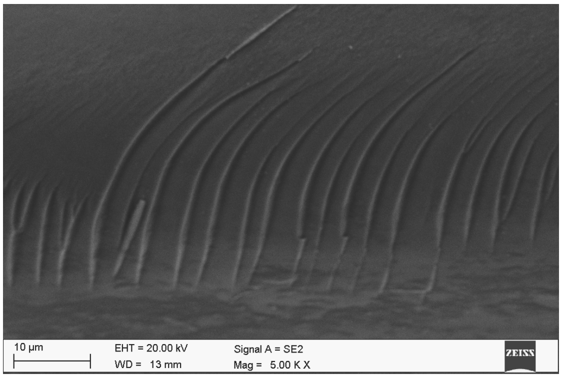

Fig. 4. SEM image of fracture surface of $Fe_{56}Co_7Ni_7B_{20}Nb_{10}$ ribbons with thickness of t=0.07 mm after decohesion; smooth fracture inside with few veins network in surface freely solidified

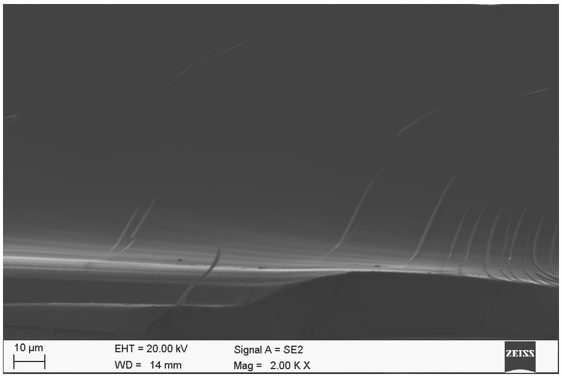

Fig. 5. SEM image of fracture surface of $Fe_{56}Co_7Ni_7B_{20}Nb_{10}$ ribbons with thickness of t=0.15 mm after decohesion; smooth fracture inside with few veins network in surface freely solidified

The microvoids content is often examined using magnetic after effects ($\Delta\mu/\mu$) measurements. The value of $\Delta\mu/\mu$ increases with the increase of microvoids in the material (Lesz, 2008). The obtained values of H_c of the ribbons with thickness of t=0.07 mm of $Fe_{56}Co_7Ni_7B_{20}Nb_{10}$ alloy are similar than in other alloys with the similar chemical composition investigated by (B. Shen, 2007) whose results for [(Fe0.8Co0.1Ni0.1)0.75B0.2Si0.05]96Nb4 alloys as follows: saturation magnetization M_s=1.1 T, coercive force H_c= 3.0 A/m (Table 1).

3. Conclusions

We can state that the ribbons of $Fe_{56}Co_7Ni_7B_{20}Nb_{10}$ alloy have an amorphous structure and good soft magnetic properties, i.e., M_s of 0.79-0.89 T, low H_c below 4 A/m. These excellent magnetic properties lead us to expect that the $Fe_{56}Co_7Ni_7B_{20}Nb_{10}$ amorphous alloy is promising for the future applications as new prominent class of engineering and functional material. Character of fracture morphology revealed ductile character of $Fe_{56}Co_7Ni_7B_{20}Nb_{10}$ ribbons with vein pattern morphology, typical for amorphous alloys.

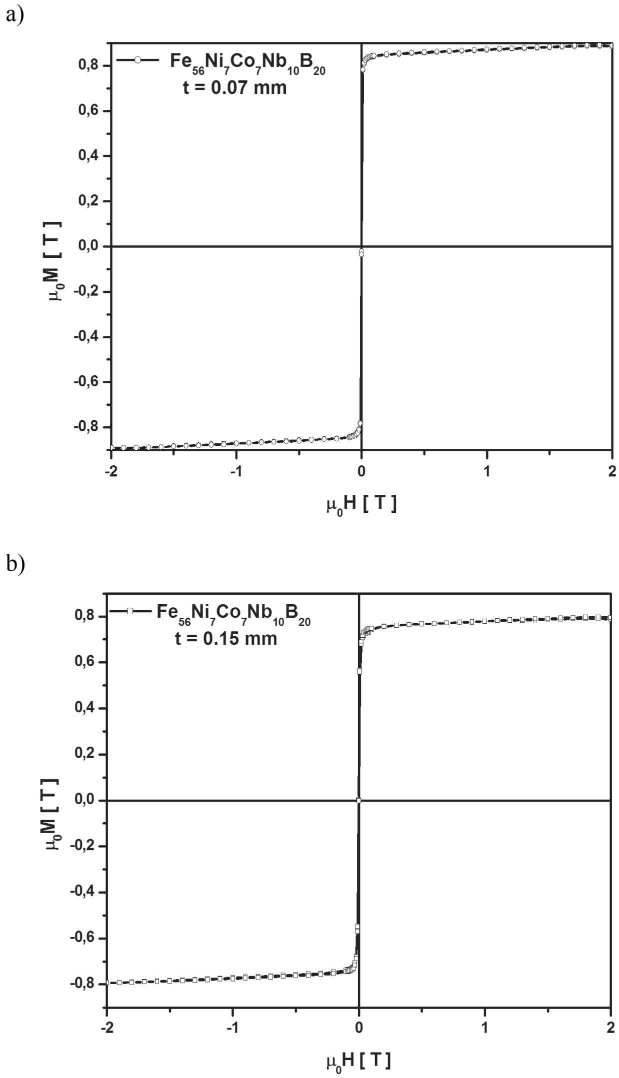

Fig. 6. Room temperature magnetic hysteresis loops measured at a maximum applied field of 2 T for $Fe_{56}Co_7Ni_7B_{20}Nb_{10}$ ribbons with thickness of t=0.07 mm (a) and t=0.15 mm (b)

References

[1] A. Inoue, A. Takeuchi, Recent development and applications of bulk glassy alloys, International Journal of Applied Glass Science 1/3 (2010) 273-295.

[2] N.P. Kovalenko, Y.P. Krasny, U. Krey, Physics of amorphous metals, Published House WILEY-VCH, Weinheim, 2001.

[3] O. Gutfleisch, M.A. Willard, E. Brück, C.H. Chen, S.G. Sankar, J.P. Liu, Magnetic materials and devices for the 21st century: stronger, lighter, and more energy efficient, Advanced Materials 23 (2011) 821-842.

[4] A.L Greer, E. Ma, Bulk metallic glasses: at the cutting edge of metals research, MRS Bulletin 32 (2007) 611-619.

[5] W. Klement, R.H. Willens, P. Duwez, Non-crystalline structure in solidified sold-silicon alloys, Nature 187 (1960) 869-870.
[6] A. Inoue, T. Zhang, H. Koshiba, A. Makino, New bulk amorphous Fe-(Co,Ni)-M-B (M=Zr,Hf,Nb,Ta,Mo,W) alloys with good soft magnetic properties, Journal of Applied Physics 83 (1998) 6326-6328.
[7] B. Shen, C. Chang, A. Inoue, Formation ductile deformation behavior and soft-magnetic properties of (Fe,Co,Ni)-B-Si-Nb bulk glassy alloys, Intermetallics 15 (2007) 9-16.
[8] A. Inoue, B.L. Shen, A new Fe-based bulk glassy alloy with outstanding mechanical properties, Advanced Materials 16 (2004) 2189-2192.
[9] D.Y. Liu, W.S. Sun, H.F. Zhang, Z.Q. Hu, Preparation, thermal stability and magnetic properties of Fe-Co-Ni-Zr-Mo-B bulk metallic glass, Intermetallic 12 (2004) 1149-1152.
[10] H.J. Sun, L. Li, Y.Z. Fang, J.X. Si, B.L. Shen, Bulk glassy $(Fe_{0.474}Co_{0.474}Nb_{0.052})_{100-x}(B_{0.8}Si_{0.2})_x$ alloys prepared using commercial raw materials, Journal of Non-Crystalline Solids 358 (2012) 911-914.
[11] Y.Z. Jia, S.Y. Zeng, S.F. Shan, L.Y. Zhang, C.Z. Fan, B.Q. Zhang, Z.J. Zhan, R.P Liu, W.K. Wang, Effect of copper addition on the glass forming ability of a Fe-Co based alloy, Journal of Alloys and Compounds 440 (2007) 113-116.
[12] PN-IEC 60050-121:2000, International Electrotechnical Vocabulary, Part 121, Electromagnetism.
[13] H. Kronmüller, Theory of magnetic after-effects in ferromagnetic amorphous alloys, Philosophical Magazine Part B 48/2 (1983) 127-150.
[14] S. Lesz, Kwapuliński, R. Nowosielski, Formation and physical properties of Fe-based bulk metallic glasses with Ni addition, Journal of Achievements in Materials and Manufacturing Engineering 31/1 (2008) 35-40.
[15] S. Lesz, R. Babilas, M. Nabiałek, M. Szota, M. Dośpiał, R. Nowosielski, The characterization of structure, thermal stability and magnetic properties of Fe-Co-B-Si-Nb bulk amorphous and nanocrystalline alloys, Journal of Alloys and Compounds 509S (2011) 197-201.
[16] A. Inoue, B.L. Shen, Soft magnetic properties of nanocrystalline Fe-Co-B-Si-Nb-Cu alloys in ribbon and bulk forms, Journal of Materials Research 18 (2003) 2799-2806.